STEM CELLS®

REGENERATIVE MEDICINE

Amniotic Fluid Stem Cells Restore the Muscle Cell Niche in a *HSA-Cre*, $Smn^{F7/F7}$ Mouse Model

MARTINA PICCOLI,[a,b] CHIARA FRANZIN,[a] ENRICA BERTIN,[a] LUCA URBANI,[a] BERT BLAAUW,[c,d] ANDREA REPELE,[a] ELISA TASCHIN,[a] ANGELO CENEDESE,[e] GIOVANNI FRANCO ZANON,[a] ISABELLE ANDRÉ-SCHMUTZ,[f] ANTONIO ROSATO,[g,h] JUDITH MELKI,[i] MARINA CAVAZZANA-CALVO,[f,j,k] MICHELA POZZOBON,[a,b] PAOLO DE COPPI[a,l]

[a]Department of Pediatrics and Pediatric Surgery, [c]Department of Physiology, [e]Department of Information Engineering, and [g]Department of Oncology and Surgical Science, University of Padova, Padova, Italy; [b]Città della Speranza Foundation, Padova, Italy; [d]Venetian Institute of Molecular Medicine (VIMM), Padova, Italy; [f]INSERM U768, Paris, France; [h]Istituto Oncologico Veneto, IRCCS, Padova, Italy; [i]INSERM U788, University of Paris 11, Hôpital Bicêtre, Le Kremlin-Bicêtre, Paris, France; [j]Département De Biothérapie, AP-HP, Hôpital Necker-Enfants Malades, Paris, France; [k]Université Paris Descartes, Faculté de Médecine, Paris, France; [l]Surgery Unit, Great Ormond Street Hospital and Institute of Child Health, University College, London, United Kingdom

Key Words. Amniotic fluid stem cells • Muscle dystrophy • Muscle stem cell niche • Spinal muscular atrophy

ABSTRACT

Mutations in the survival of motor neuron gene (*SMN1*) are responsible for spinal muscular atrophy, a fatal neuromuscular disorder. Mice carrying a homozygous deletion of *Smn* exon 7 directed to skeletal muscle (*HSA-Cre,* $Smn^{F7/F7}$ mice) present clinical features of human muscular dystrophies for which new therapeutic approaches are highly warranted. Herein we demonstrate that tail vein transplantation of mouse amniotic fluid stem (AFS) cells enhances the muscle strength and improves the survival rate of the affected animals. Second, after cardiotoxin injury of the *Tibialis Anterior*, only AFS-transplanted mice efficiently regenerate. Most importantly, secondary transplants of satellite cells (SCs) derived from treated mice show that AFS cells integrate into the muscle stem cell compartment and have long-term muscle regeneration capacity indistinguishable from that of wild-type-derived SC. This is the first study demonstrating the functional and stable integration of AFS cells into the skeletal muscle, highlighting their value as cell source for the treatment of muscular dystrophies. STEM CELLS *2012; 30:1675–1684*

Disclosure of potential conflicts of interest is found at the end of this article.

INTRODUCTION

In the last few years, we and others have focused on the characterization of c-kit$^+$ stem cells isolated from human and mouse amniotic fluid [1–3]. Amniotic fluid stem (AFS) cells are broadly multipotent [1] and are able to repopulate the bone marrow (BM) when transplanted into immunocompromised animals [3], while differing from pluripotent stem cells because of their inability to form teratomas [1]. AFS cells have been tested in various disease models and have been shown to contribute to lung [4], kidney [5, 6], cardiac [7], and smooth muscle regeneration [8]. They can also generate myotubes in vitro [1], but very little is known about their potential to functionally engraft into regenerating skeletal muscle [9]. So far, freshly isolated satellite cells (SCs), which are postnatally responsible of both de novo muscle formation and repair, showed the best myogenic potential, even if they are limited in number and do not engraft when injected systemically [10–12]. Although alternative cell sources have been explored, replacement of stem cells in damaged or diseased skeletal muscles remains an unsolved problem. In this context, AFS cells may have broader differentiative potential than adult stem cells and, similarly to BM cells, mesangioblasts [13–15], and pericytes [16], can cross the endothelial barrier and are therefore suitable for systemic injection [4, 17].

In order to test the hypothesis that AFS cells could functionally engraft in a diseased muscle, we used a mouse model of spinal muscular atrophy, in which the phenotypic disease is full blown in muscle tissue [18]. In this model, the murine *Smn* exon 7 is flanked by two LoxP sequences (Smn^{F7}) and deletion is occurring only in skeletal myofibers by placing the

Author contributions: M.P., M.P., and P.D.C: conception and design, data analysis and interpretation, and manuscript writing; C.F.: conception and design, animals genotyping, and data analysis and interpretation; E.B.: collection of amniotic fluid samples; L.U.: collection of muscle samples and data analysis and interpretation; B.B.: muscle mechanics analyses; A.R.: collection of muscle samples; E.T.: animals genotyping; A.C.: image processing; G.F.Z.: financial support; I.A.-S.: data analysis and interpretation; A.R.: in vivo imaging; J.M.: animal model provider; M.C.-C.: data analysis and interpretation and manuscript writing. M.P. and P.D.C. contributed equally to this article.

Correspondence: Michela Pozzobon, Ph.D., Città della Speranza Foundation, Viale della Ricerca scientifica, 35127 Padova, Italy. Telephone: +39 0445 602972; Fax: + 39 0445 584070; e-mail: m.pozzobon@cittadellasperanza.org; or Paolo De Coppi, M.D., Ph.D., Surgery Unit, UCL Institute of Child Health, 30 Guilford Street, London WC1N 1EH, U.K.. Telephone: +44(0)2079052808; Fax: +44(0)2074046181; e-mail: p.decoppi@ich.ucl.ac.uk Received December 6, 2011; accepted for publication May 12, 2012; first published online in STEM CELLS *EXPRESS* May 29, 2012. 1066-5099/2012/$30.00/0 doi: 10.1002/stem.1134

Cre recombinase under the control of the human α-skeletal actin gene promoter (*HSA-Cre*). Similarly to other models of muscle disease, *HSA-Cre, Smn$^{F7/F7}$* mice display a high proportion of myofibers with central nuclei, which lead with time to muscle fibers necrosis, heterogeneous myofiber diameters, and infiltration of interstitial tissue [18]. In contrast to the *mdx* mouse model, *HSA-Cre, Smn$^{F7/F7}$* animals manifest kyphosis, progressive muscle weakness, shrinkage, and subsequent respiratory arrest, similarly to the clinical features exhibited by the *mdx*/*mTR* mouse model [19]. Therefore, the overall survival of *HSA-Cre, Smn$^{F7/F7}$* animals is estimated to be of 10 months. After BM transplantation, the myopathic phenotype attenuates and the myofibers number and motor performance normalize up to 9 months of age [20]. However, the engraftment in the diseased muscle tissue is poor: the cells are not able to rescue the phenotype and make a substantial, long-term therapeutic contribution [20]. Hence, the aim of this work was to establish whether AFS cells transplantation would produce physiologically and functionally significant skeletal muscle repair in the *HSA-Cre, Smn$^{F7/F7}$* mouse.

Materials and Methods

Mice

Male C57BL/6 (Ly5.2) GFP$^{+/-}$ mice and female C57BL/6 (Ly5.2) GFP$^{-/-}$ mice were used to obtain both Ly5.2 GFP$^{+/-}$ and GFP$^{-/-}$ embryos. *HSA-Cre, Smn$^{F7/F7}$* mice were used as recipients. All procedures were approved by the University of Padua's Animal Care and Use Committee (CEASA, protocol references 107/07 and 41056) and, in accordance with Italian law, were communicated to the Ministry of Health and local authorities.

Amniotic Fluid Collection and Stem Cell Selection

Embryo age was defined relative to the morning of vaginal plug discovery (E0.5). All dissections were performed under a stereomicroscope (Leica Microsystems, Milano, Italy). Amniotic fluid samples from F1 embryos were harvested from pregnant mice between embryonic days E11.5 and E13.5, as described elsewhere [3]. Murine amniotic fluid-derived c-kit$^+$ cells were isolated using the Miltenyi Mouse Lineage Cell depletion kit and then CD117 MicroBeads (all from Miltenyi Biotech, Bologna, Italy). The freshly isolated murine AFS cells constituted a heterogeneous population of cells characterized by the presence of cell markers such as CD90, CD44, Ly5.2 (CD45.2), Sca1, and CD105 (Supporting Information Fig. S1 and Ditadi et al. [3]).

BM Collection

Wild-type (WT) BM cells were isolated under sterile conditions from 6- to 10-week-old isogenic mice that ubiquitously expressed green fluorescent protein (GFP). The femur and tibia were surgically removed and placed in Dulbecco's modified Eagle's medium (DMEM) culture medium with 10% fetal bovine serum (FBS) (Gibco, Milano, Italy). Marrow was collected and red blood cells were lysed with 0.75% NH_4Cl in 20 mM Tris, pH 7.2.

AFS Cell Expansion

After selection, freshly isolated AFS cells were plated onto a feeder layer of mitomycin C-treated mouse embryonic fibroblasts in DMEM knockout (Invitrogen, Milano, Italy) supplemented with 15% heat-inactivated FBS, 100 mM nonessential amino acids (Invitrogen), 2 mM L-glutamine (Sigma, Milano, Italy), 50 units/ml penicillin (Sigma), 50 mg/ml streptomycin (Sigma), 0.01 mM 2-mercaptoethanol (Sigma), 20 ng/ml stem cell factor (SCF) (Peprotech), 10 ng/ml bone morphogenetic protein 4 (BMP4) (R&D Systems, Minneapolis, USA), and 20 ng/ml leukemia inhibitory factor (LIF) (Sigma). Cells were cultivated at 37°C and 5% CO_2.

Cell Injection

Three-month-old *HSA-Cre, Smn$^{F7/F7}$* mice were randomized to receive either no treatment (control group, group I), BM cells (group II), or AFS cells (group III). Approximately 25,000 GFP$^+$ cells were injected via tail vein in the AFS cells group ($n = 40$) and approximately 50,000 GFP$^+$ cells were injected via tail vein in the BM group ($n = 20$). In vitro expanded AFS cells were sorted with an Aria FACS system (Becton Dickinson, Milano, Italy) and selected for the expression of GFP and c-kit prior to injection (25,000 AFS cells, $n = 6$). After sacrifice (1 or 15 months post-transplantation [pt]), muscle differentiation and regeneration were investigated by assessing the percentage of cells derived from donor GFP$^+$ cells in recipient muscles, considering the total number of muscle fibers (both centrally nucleated and with peripheral nuclei). In animals treated with AFS cells ($n = 6$) or BM cells ($n = 6$), the *Tibialis Anterior* (*TA*) muscles were injured 1-month pt by injection of 10 μM cardiotoxin (Sigma). Muscle regeneration was analyzed 15 days after injury, that is, 45 days pt.

Secondary Transplants

Single myofibers were isolated from BM- and AFS-transplanted animals and from C57BL/6 GFP$^+$ mice, as previously described [12, 21]. Briefly, *extensor digitorum longus* (*EDL*) and *Soleus* muscle were digested for 2 hours at 37°C in 0.2% (wt/vol) type I collagenase (Sigma-Aldrich), reconstituted in DMEM (high glucose, with L-glutamine, supplemented with 1% penicillin-streptomycin; Invitrogen). Following digestion, muscles were transferred in DMEM (low glucose; Invitrogen) on a horse serum (Invitrogen)-coated 10-cm dish (Falcon; BD Biosciences) and gently triturated with a wide-bore pipette to release single myofibers. Fresh SCs were stripped off the fibers by repeated passage through an 18-gauge needle. Five hundred cells were injected locally into *TA* of naive, 3-month-old *HSA-Cre, Smn$^{F7/F7}$* mice. Animals were sacrificed 1-month pt.

Muscle Physiology, Histology, and Immunofluorescence Analyses

In vivo determination of *gastrocnemius* strength and contraction kinetics was carried out as described previously [22]. Transverse sections (8–10-μm thick) of isopentane-frozen skeletal muscle including *TA*, *gastrocnemius*, *EDL*, and diaphragm of 3-month-old transplanted mice were stained with hematoxylin and eosin and Masson's trichrome. To evaluate the total number of centrally nucleated muscle fibers, serial 400-μm sections of the entire *TA* muscle were prepared. Immunostaining of GFP or dystrophin was performed using rabbit anti-GFP (1:200; Invitrogen) or anti-dystrophin (1:150; Abcam, Cambridge, UK). Sections were mounted with Vectashield and 4,6-diamidino-2-phenylindole (Dapi) (Vector Laboratories, Peterborough, UK), observed under an Olympus BX60 microscope (Olympus), and pictures taken using Viewfinder Lite software.

In Vivo Imaging

Prior to imaging, mice were anesthetized (with a mixture of Rompum and Zoletil given i.p.), shaved and depilated to completely remove hair, and imaged on the eXplore Optix time-domain imager (ART, Montreal, Quebec). Image processing and data analysis were performed using eXplore Optiview 1.04 software (ART).

DNA Extraction and PCR Analyses

DNA from organ and tissues samples was extracted with a DNeasy Blood & Tissue kit (QIAGEN GmbH, Milano, Italy) and then quantified with a ND-1000 spectrophotometer (Thermo Scientific, Waltham, MA, USA). Genomic DNA samples extracted from GFP$^+$ AFS cells and from WT organs were, respectively, used as positive and negative controls for the amplification of the *GFP* gene. Polymerase chain reaction (PCR) reactions for the *TERT* and *GFP* genes were carried out as previously described [17].

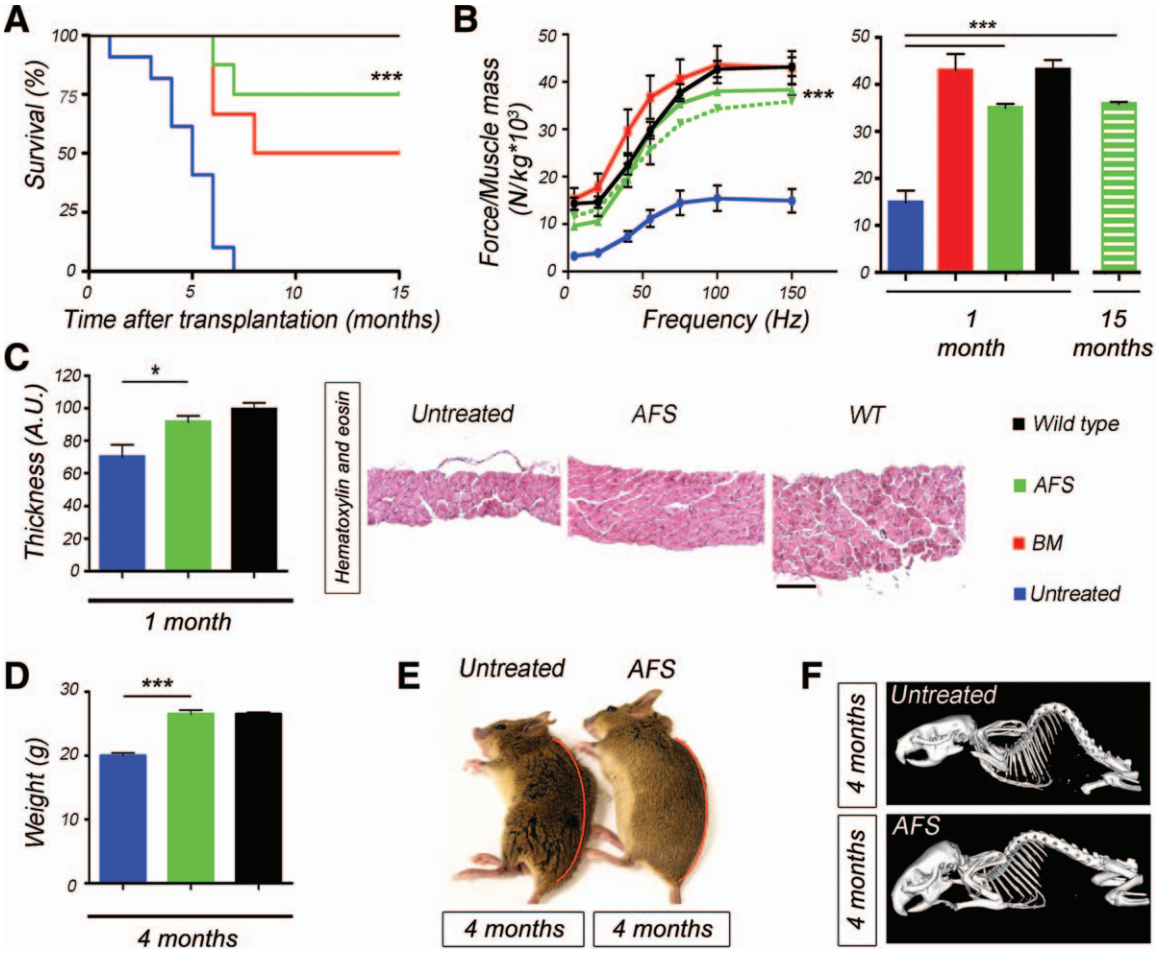

Figure 1. Transplanted animals improve in survival and clinical parameter. **(A):** Survival curve: AFS-treated mice increased life expectancy both when compared with BM-treated and -untreated animals. Untreated = 10 animals, BM = eight animals, AFS = eight animals (***, $p < .001$). **(B):** Left panel: muscle strength analyzed at different frequencies; right panel: mean value of muscle strength analyzed at 150 Hz of frequency. Normalized force frequency on muscle mass displays that both BM- ($n = 8$) and AFS-treated ($n = 8$) mice had 75% more muscle strength than untreated ($n = 6$) animals 1 month after transplantation (***, $p < .001$). AFS-treated animals analyzed at 18 months of age (green dotted line; $n = 4$). **(C):** Diaphragm thickness 1 month after transplantation ($n = 3$ per group), in AFS-treated animals was similar to age-matched wild-type animals while they are both distinct from untreated animals (scale bar = 100 μm; *, $p < .05$). **(D):** Bodyweight of untreated ($n = 4$), AFS-treated ($n = 4$), and WT ($n = 8$) mice at 8 months (***, $p < .001$). **(E):** The kyphosis, which is present in the untreated mice from 3 months of age, disappeared in AFS-treated mice. **(F):** MicroCT scan of skeletal anatomy of untreated and AFS-treated mice confirmed the different curvature of the spine. Abbreviations: AFS, amniotic fluid stem; BM, bone marrow; WT, wild type.

Real Time PCR

In order to quantify the different amount of *Pax7*, *MyoD*, *MRF4*, *Myf5*, and *Myogenin* mRNAs in muscles and freshly isolated cells, total RNA has been extracted using RNeasy Plus Mini kit (QIAGEN GmbH) following the supplier's instructions. RNA has been then quantified with a ND-1000 spectrophotometer and 1 μg has been retrotranscripted with SuperScript II and related products (all from Invitrogen) in a 20 μl reaction. Real-time PCR (RT-PCR) reactions were performed using a LightCycler II (Roche, Monza, Italy). Reactions have been carried out in triplicate using 4 μl of FASTSTART SYBR GREEN MASTER (Roche) and 2 μl of primers mix FW + REV (final concentration, 300/300 nM) in a final volume of 20 μl. Serial dilutions of a positive control sample have been used to create a standard curve for the relative quantification. The amount of each mRNA has been normalized for the content in β_2-*microglobulin*.

Statistical Analyses

Data are expressed as means ± SEM or as means ± SD. For immunofluorescence, immunohistochemical, and regeneration index analyses, 15 random high-power field areas were considered per each analyzed muscle. Statistical significance was determined using an equal-variance Student's *t* test, two-way analysis of variance (ANOVA) test, a log-rank test (for survival curves), and the Mann–Whitney *U* test (for quantitative real time-polymerase chain reaction [qRT-PCR] analyses). A *p* value below .05 was considered to be statistically significant.

Results

AFS Cell Transplantation Ameliorates Clinical Course and Strength Recovery

At the age of 3 months, mutant mice (*HSA-Cre, Smn*$^{F7/F7}$) were randomized to receive via tail vein GFP$^+$ AFS cells (25,000 cells, $n = 40$), GFP$^+$ BM cells (50,000 cells, $n = 20$), or no treatment (untreated, $n = 20$) (Supporting Information Table S1). AFS cells were derived and characterized (Supporting Information Fig. S1A) as previously described [3, 20]. As expected, all untreated animals died by the age of 10

months, whereas the BM- and AFS-treated groups had at that time survival rates of 50% and 75% ($p < .001$), respectively (Fig. 1A). The treated mice dramatically differed from the untreated animals: *gastrocnemius* contraction kinetics was measured blinded 1-month pt as previously described [22] and confirmed that both BM- and AFS-treated mice achieved levels of strength comparable to the ones obtained with WT mice (Fig. 1B). Remarkably, the AFS-treated animals, which survived until 15 months pt (i.e., 18 months of age), maintained the strength acquired at 1-month pt (Fig. 1B). Consistently with survival and muscle strength, AFS-treated mice were similar to WT mice in terms of diaphragm thickness, weight, movement, and skeletal anatomy as confirmed at MicroCT scan analysis (Fig. 1C--1F). On the contrary, *HSA-Cre, Smn$^{F7/F7}$*, which did not receive any treatment, showed typical thinner diseased diaphragmatic muscles at 4 months of age (Fig. 1C) and pronounced kyphosis with impaired movements by the age of 8 months (Fig. 1D--1F). When fiber diameter was measured, at first both AFS- and BM-treated muscles demonstrated a normalization of dimensions close to WT muscle; notably in the long-term experiments this normalization was maintained only by the AFS-treated muscles, while those treated with BM had very large hypertrophic fibers (Supporting Information Fig. S2, [23]).

Transplantation of AFS Cells Leads to Restoration of Muscle Phenotype in Mutant Mice

Following morphological muscle analyses performed 1-month pt (i.e., 4 months of age; Fig. 2A), in both BM- and AFS-treated mice, the histological aspect of the muscle tissue resulted indistinguishable from WT, with few central nucleated fibers (<1%, comparable to WT mice; Fig. 2B, 2F, 2G). In contrast, untreated animals presented a very large number of central nucleated fibers (mean value: 63.70% ± 0.41%, $p < .001$; Fig. 2B, 2F, 2G). Masson's trichrome staining showed that untreated animals presented large connective tissue areas between fibers, which were absent in both WT and cell-treated mice. Immunofluorescence analyses clearly indicated that the morphological appearance of muscle in BM- and AFS-treated animals was correlated with a relevant proportion of GFP$^+$ fibers (31.57% ± 7.04% and 37.86% ± 9.48%, respectively; Fig. 2G). It is worth of notice that in this particular muscular model, the beneficial effect of AFS cells transplantation is detectable very soon after injection. In fact, only 12 hours after injection the number of centrally nucleated fiber greatly diminished (7.90% ± 2.31%) to look similar to WT muscle only after 7 days (0.53% ± 0.09%; Supporting Information Fig. S3). Importantly, this in vivo effect did not relate to the presence of myogenic precursors in the transplanted populations, which was excluded by demonstrating that the myogenic genes *Pax7*, *MyoD*, *Myf5*, *Mrf4*, and *Myogenin* were neither expressed in freshly isolated BM nor expressed in AFS cells (Supporting Information Fig. S1B). Last, massive changes in the muscle tissue were also confirmed by the observed distribution of dystrophin expression, which was similar only in transplanted and WT mice but differed in the untreated animals (Fig. 2B). It was not possible to consider the restoring of the Smn protein as amelioration in the transplanted animals since Smn is expressed also in the *HSA-Cre, Smn$^{F7/F7}$*mice [18].

Despite the similarity between BM- and AFS-treated animals in terms of physiology and number of central nucleated and GFP$^+$ myofibers, the engraftment index, defined as the number of donor-engrafted myofibers generated per 10^5 transplanted cells [4], differed significantly between BM- (1,263.00 ± 282.76) and AFS-treated mice (3,029.16 ± 758.71; $p < .001$), respectively (Fig. 2C). Additionally, qRT-PCR revealed that 1 month after treatment, in the *TA* muscles of AFS-treated mice, there was higher expression of *Pax7* than in untreated or BM-treated mice ($p < .05$; Fig. 2D). Further evidence of the differences between the two groups was confirmed by analysis of surviving animals at 15 months pt (Fig. 2A). Morphological analysis of samples from BM-treated mice displayed a high number of central nucleated fibers (39.90% ± 17.68%) and consistent infiltration of interstitial tissue between the myofibers—a situation that differed greatly from the one observed in AFS-treated mice (Fig. 2E--2G). Moreover, at this stage (15 months pt), no GFP$^+$ fibers were found in BM-treated animals, whereas 58.00% ± 2.43% of myofibers were GFP$^+$ in AFS-treated mice (Fig. 2E--2G). This finding highlights the sustained effect of AFS cells transplantation. PCR analyses of GFP expression performed 1 and 15 months pt proved that the AFS cells were able to engraft systemically throughout various skeletal muscles (Supporting Information Fig. S4A) and this was also confirmed after Western blot was performed in muscles (Supporting Information Fig. S4B). The ability of AFS cells to engraft various skeletal muscle tissues was also validated by the fact that both the number of central nucleated and GFP$^+$ fibers were comparable among *gastrocnemius*, *EDL*, and diaphragm at 1-month pt, with GFP$^+$ fibers variation from 17.28% ± 3.66% for diaphragm to 38.52% ± 6.87% for *EDL* (Supporting Information Fig. S4C). Differently, this could also be explained by the migratory potential of AFS cells that is consistent, besides the skeletal muscle territory, with the multiple organ engraftment similar to the one observed after systemic injection of human AFS cells [4] (Supporting Information Fig. S4D).

AFS Cells Engraft in the Muscle Stem Cell Niche

Since AFS cells were able to sustain long-term muscle regeneration, we assume that they were able to integrate into the muscle stem cell niche. In AFS-treated muscles, GFP$^+$ cells were found in sublaminal position, which was evident also when fibers were isolated in culture (Fig. 3A, 3B). Moreover, some of these cells costained for Pax7 and alpha7integrin (a7int) both when adherent to the fiber and after stripping (Fig. 3C--3E).

To confirm functional integration of AFS cells in the muscle stem cell niche, both cardiotoxin injury and secondary transplants experiments were performed. In a first set of experiments, cardiotoxin was injected into the *TA* of BM- and AFS-treated mice 1 month after systemic cell transplantation (Fig. 4A). Only AFS-treated mice showed newly regenerating GFP$^+$ muscle fibers (51.75% ± 1.35%; Fig. 4B, 4D) when analyzed 45 days pt, whereas no GFP$^+$ fibers were observed in animals transplanted with BM cells (Fig. 4B, 4D). Moreover, almost all fibers in AFS-transplanted mice were perinucleated before and after damage with cardiotoxin (Supporting Information Fig. S5). On the contrary, after injury of BM-treated mice, 38.07% ± 2.54% of the regenerating fibers was centrally nucleated (Fig. 4B, 4C) confirming that only AFS cells were capable of restoring physiological muscle conditions.

To exclude that AFS cells potential to regenerate skeletal muscle even after cardiotoxin injury was simply related to their fetal origin, c-kit$^+$ fetal liver (FL) cells were used as further control. Interestingly, c-kit$^+$ FL cells did not differ from BM cells and GFP$^+$ fibers were not found after cardiotoxin injury confirming the unique muscle regeneration potential of AFS cells (Supporting Information Fig. S6).

To further establish whether AFS cells were truly engrafted into the muscle niche and replaced resident muscle stem cells, secondary transplants were performed (Fig. 4A). Single myofibers were isolated from BM- ($n = 6$) and AFS-

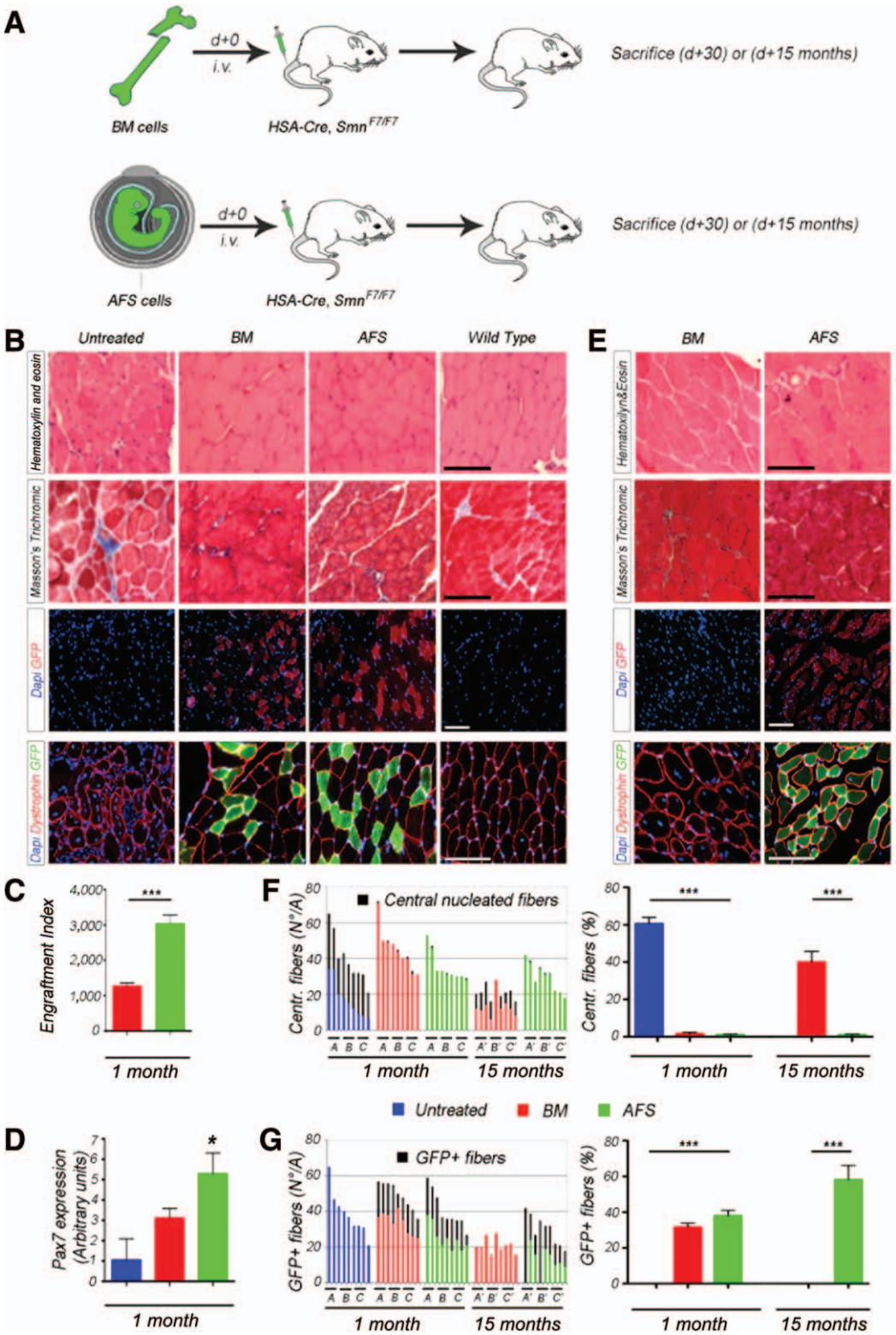

Figure 2. Restoration of muscle phenotype in mutant mice. **(A):** Three-month-old *HSA-Cre*, $Smn^{F7/F7}$ mice were transplanted alternatively with BM or AFS cells and sacrificed 1 month after treatment for analyses. **(B):** One month after transplantation, hematoxylin and eosin staining reveals a normal appearance of the *Tibialis Anterior* (*TA*) muscle structure after receiving either BM or AFS cells. On the contrary, *TA* muscle of untreated animals present fibers disarrangement (dystrophin staining) with interstitial tissue deposition identified at Masson's trichrome. Scale bar = 100 μm. **(C):** Engraftment index indicates that AFS cells are more likely to participate in muscle regeneration than BM cells;***, $p < .001$. **(D):** Quantitative real time-polymerase chain reaction (PCR) for *Pax7* expression revealed that mutant muscles receiving AFS cells ($n = 3$) expressed higher levels of *Pax7* than untreated ($n = 3$) and BM ($n = 3$) animals; *, $p < .05$. **(E):** Fifteen months after transplantation, histological and immunofluorescence analyses revealed a more sustained, long-term engraftment of AFS cells, relative to BM cells. Scale bar = 100 μm. **(F, G):** Graphs of raw numbers (number of fibers per area [*N/A*]; each letter on the *x*-axis is an individual muscle evaluated in three representative high-power fields) and percentages of central nucleated and GFP^+ fibers (black) in untreated (blue), BM (red), and AFS-treated (green) mice at 1 and 15 months after transplantation; ***, $p < .001$. Abbreviations: AFS, amniotic fluid stem; BM, bone marrow; GFP, green fluorescent protein.

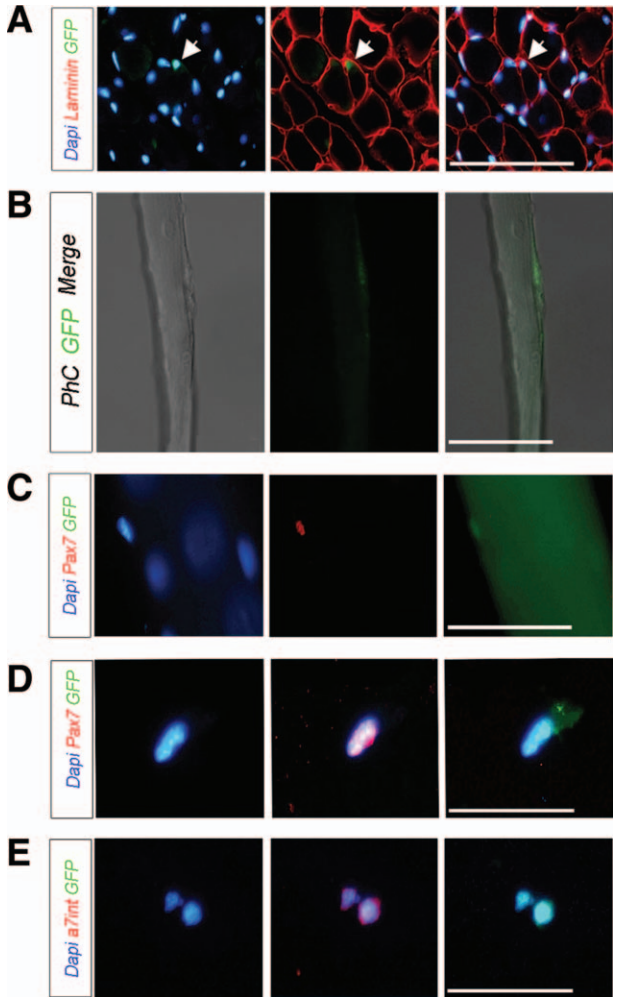

Figure 3. Amniotic fluid stem (AFS) cells differentiate in muscle stem cells. **(A):** Immunofluorescence of *Tibialis Anterior* (*TA*) muscle from AFS-treated mouse; GFP^+ cells are localized in the subliminal zone (GFP in green, laminin in red). **(B):** Detection of GFP^+ cells in isolated fiber. **(C):** Immunofluorescence of Pax7 (red) and GFP (green) in fiber isolated from *TA* muscle of AFS-treated animal. **(D, E):** Cytospin of satellite cell isolated from *TA* muscle of AFS-treated mouse. Coexpression of Pax7 and alpha7 integrin with GFP demonstrated the differentiation of AFS cells in muscle stem cells. Scale bars = 100 μm. Abbreviation: GFP, green fluorescent protein.

($n = 6$) transplanted animals and from WT C57BL/6 GFP^+ mice ($n = 3$), as previously described [12, 21]. Five hundred freshly isolated SCs, disengaged from single myofibers, were injected locally into *TA* muscles of naive, 3-month-old *HSA-Cre, $Smn^{F7/F7}$* mice. One month after secondary transplantation, all the mice in the AFS cell group ($n = 6$) had GFP^+ fibers (mean: 31.47% ± 2.63%; Fig. 4E, 4F) and did not differ significantly in this respect from hosts having received WT GFP^+ SCs (mean 32.21% ± 3.39%; Fig. 4E, 4F). In contrast, only one out of six of the recipients of muscle cells derived from BM-treated mice had a few GFP^+ fibers (4.80% ± 3.86%). Furthermore, this expression pattern was confirmed by molecular analyses of *GFP* genomic DNA expression in *TA* muscles of the secondary transplanted animals (Fig. 4G).

Expanded AFS Cells Preserve Myogenic Potential

Given the poor recovery of freshly isolated AFS cells and the strong therapeutic interest, we explored the myogenic potential of ex vivo-expanded AFS cells (Fig. 5A). After 2 weeks of culture on a fibroblast feeder layer (Fig. 5B), AFS cells were sorted for the dual expression of GFP and c-kit (89.50% ± 6.27%) and then transplanted in 3-month-old *HSA-Cre, $Smn^{F7/F7}$* mice. Similarly to what had been observed with the freshly isolated AFS cells, the muscles of treated mice displayed, 1 month after treatment, a normal phenotype with well-organized dystrophin expression, less than 1% centrally nucleated fibers, and 21.01% ± 3.57% GFP^+ fibers (Fig. 5C, 5D). Multiple skeletal muscle engraftments in the transplanted animals were also confirmed by PCR analyses of *GFP* expression (Fig. 5E).

Discussion

Our results strongly suggest that AFS cells, but not BM cells, integrate in the muscle stem cell compartment and have long-term potential for muscle regeneration in *HSA-Cre, $Smn^{F7/F7}$* mutant mice. This mouse model, which has been extensively characterized, closely replicates the clinical features of human muscular dystrophies. When injected systemically into *HSA-Cre, $Smn^{F7/F7}$* mutant mice, BM cells were not able to rescue the phenotype and have shown a limited therapeutic efficiency failing to make a substantial, long-term therapeutic contribution [20].

Unselected and selected BM cell populations have been widely tested in various mouse models of muscle diseases, with an initial enthusiasm prompted by the cells' ability to fuse with the host muscle tissue [24, 25] and subsequently activate resident SCs [20]. However, it is still not clear whether BM cells are able to integrate in the muscle stem cell niche and are capable of regenerating neofibers after damage [26, 27]. Mesenchymal stem cells from BM and other sources are able to restore dystrophin expression in the *mdx* mouse, but the impact on muscle repair is dependent on forced expression of MyoD [28–30]. BM stem cells may indeed be therapeutic by producing molecules that regulate muscle regeneration [2] or reduce inflammation [3], while they are able to establish immune tolerance in a dystrophic animal model and allow stable engraftment of donor muscle-derived cells [31].

More encouraging results have been obtained using stem cells isolated directly from muscle tissue. The intra-arterial delivery of niche-derived mesangioblasts results in the morphological and functional correction of the dystrophic phenotype in adult immunocompetent α-sarcoglycan null mice [32], in SCID/BlAJ mice, a novel model of dysferlinopathy [33], and golden retriever muscular dystrophy dogs [14]. Alternatively, functional myogenic cells can be also derived from embryonic stem cells (ESCs) [34]. Intramuscular and systemic transplantation of $Pax3^+$ $PDGF\text{-}\alpha R^+$ and $Flk1^+$ ES-derived cells into dystrophic mice results in extensive engraftment of adult myofibers, with enhanced contractile function and no teratoma formation [35]. In order to overcome the immunological problem related to ESCs transplantation, patient-specific induced pluripotent stem (iPS) cells could also be generated [36]. Similarly to ESCs, iPS cells can both generate in vitro skeletal muscle stem cells, and, after enrichment using the anti-SC antibody SM/C-2.6, functionally engraft into skeletal muscle when transplanted into *mdx* mice [37, 38]. While ES- and iPS-derived myogenic cells may become useful for therapy in the future, a readily available source of cells with myogenic potential would be relevant as therapeutic alternative to muscle-derived stem cells.

Our group has previously demonstrated that (a) broadly multipotent stem cells can be derived from amniotic fluid [1]

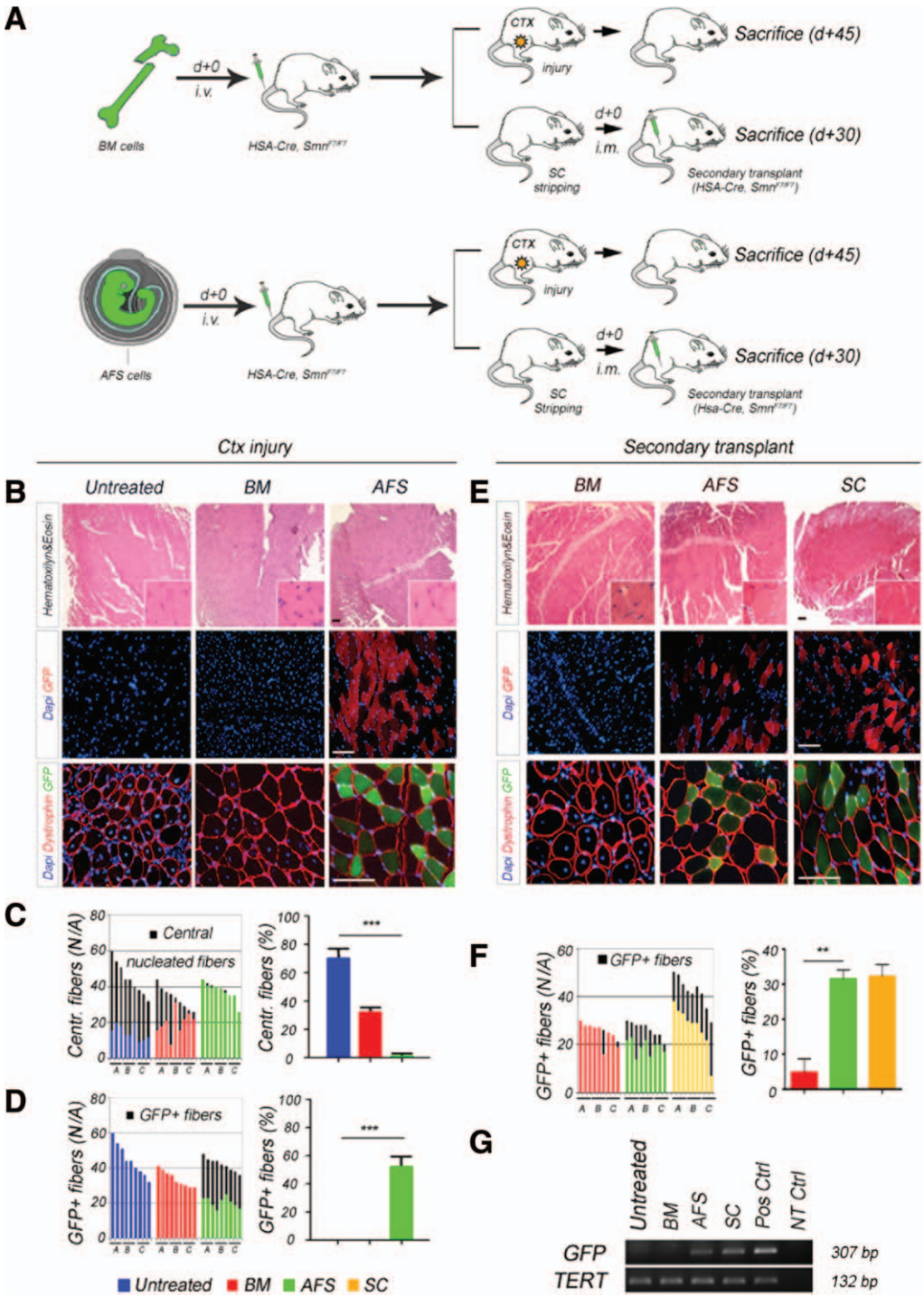

Figure 4. AFS cells fill the muscle stem cell niche. **(A):** *Tibialis Anterior* (*TA*) muscles of BM- and AFS-treated mice were injured with cardiotoxin (Ctx) 30 days post-transplantation (pt) and animals were sacrificed 45 days pt. For secondary transplant experiments, primary transplanted mice were sacrificed 30 days pt, SCs were isolated from the *extensor digitorum longus* and *Soleus* muscles and injected into secondary *HSA-Cre, Smn*$^{F7/F7}$ hosts, which were sacrificed and analyzed 30 days later. **(B--D):** Ctx injury: 15 days after Ctx injury, only AFS-treated mice displayed GFP$^+$ fibers. Graphs of raw number and percentages of central nucleated (untreated 63.70 ± 3.24; BM-treated 38.07% ± 6.73%; AFS-treated <0.1%; ***, $p < .001$) and GFP$^+$ fibers (untreated 0%; BM-treated 0%; AFS-treated 51.75% ± 1.35%; ***, $p < .001$) in untreated, BM- and AFS-treated mice demonstrated that only AFS cells efficiently regenerate skeletal muscle fibers. **(E, F):** Secondary transplants: 30 days pt, GFP$^+$ fibers were observed in all six mice injected with SC derived from AFS-treated mice (31.47% ± 2.63%), but only in one out of six mice transplanted with SC derived from BM-treated mice (4.80% ± 3.86%; **, $p < .01$). Scale bar = 100 μm. A, B, and C letters on the x-axis in graphs (C), (D) and (F) represent an individual muscle evaluated in three representative high-power fields. **(G):** PCR analysis confirmed that *TA* muscle treated with SC isolated from primary AFS-treated mice expressed GFP. Amplification of the *GFP* gene (307 bp) and *TERT*, telomerase reverse transcriptase (132 bp) in *TA* muscles of untreated, secondary BM-treated (BM), secondary AFS-treated (AFS), and GFP$^+$ SC-treated (SC) *HSA-Cre, Smn*$^{F7/F7}$ mice (Pos Ctrl: genomic DNA from GFP$^+$ AFS cells). Abbreviations: AFS, amniotic fluid stem; BM, bone marrow; GFP, green fluorescent protein; NT Ctrl, no template control; Pos Ctrl, positive control; SCs, satellite cells.

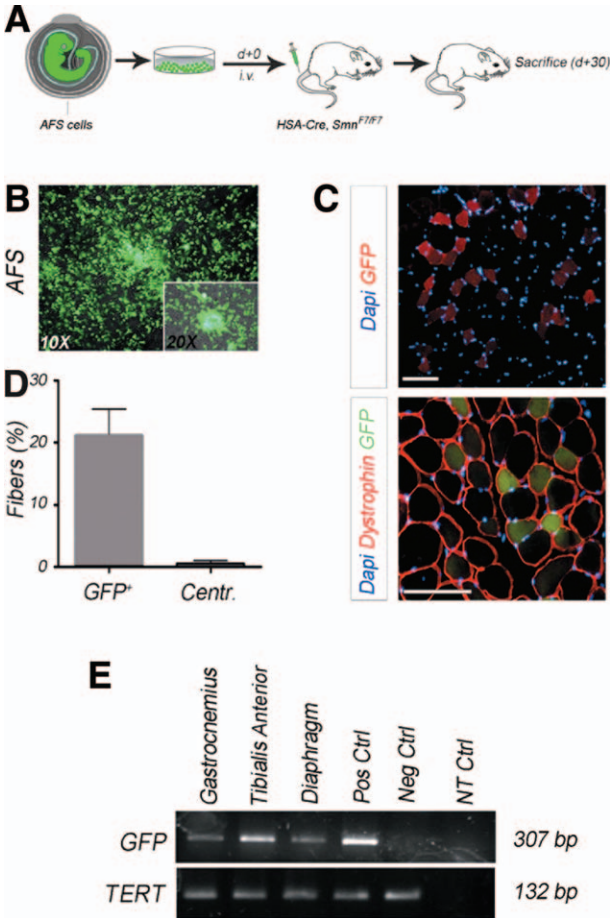

Figure 5. Transplantation of expanded AFS cells generates skeletal muscle tissue. **(A):** After 15 days of culture, AFS cells GFP$^+$/c-kit$^+$ were sorted and injected in *HSA-Cre, Smn*$^{F7/F7}$ mice. **(B):** GFP$^+$ AFS cells were passaged twice on a mouse embryonic fibroblast feeder layer. Magnification ×10 and ×20 for the inset. **(C):** Immunofluorescence with anti-GFP and antidystrophin antibodies: 1 month after transplantation, the muscles of treated *HSA-Cre, Smn*$^{F7/F7}$ mice displayed a considerable number of GFP$^+$ fibers and a normal level of dystrophin expression. Scale bar = 100 μm. **(D):** Percentage of GFP$^+$ and central nucleated myofibers in cultured AFS-treated animals. **(E):** PCR analyses of *gastrocnemius*, *Tibialis Anterior*, and diaphragm muscles isolated from mice transplanted with cultured AFS cells. First lane: amplification of the *GFP* gene (307 bp). Second lane: amplification of genomic *TERT* (132 bp) to confirm the quality of the extracted DNA. For each PCR, the Pos Ctrl for GFP amplification was the genomic DNA extracted from GFP$^+$ AFS cells. Abbreviations: AFS, amniotic fluid stem; GFP, green fluorescent protein; Neg Ctrl, negative control; NT Ctrl, no template control; Pos Ctrl, positive control.

and (b) freshly isolated murine AFS cells show hematopoietic potential when injected in Rag1$^{-/-}$ mice [3]. AFS cells have been tested in various disease models and have been shown to contribute to organ regeneration [4, 5, 7]. Similarly to BM cells and mesangioblasts [14], AFS cells can cross the endothelial barrier and are therefore suitable for systemic injection [4, 17]. However, their myogenic potential remains to be fully elucidated.

While AFS cells have shown to be able to fuse into myotubes [1], Gekas et al. failed to show functional engraftment of human AFS cells after expansion when injected in immunocompromised animals [9]. Differently, we show here for the first time that murine AFS cells are able to restore muscle function in a model of disease and to maintain their efficient therapeutic effect with time possibly because of their unique ability of switching to muscle stem cells. The beneficial effects are tightly correlated with normalization of pathological skeletal muscle regeneration and the remarkable attenuation of the mutant phenotype (treated animals shown neither kyphosis nor abdominal shrink)—resulting in the long-term survival observed here.

We first hypothesized that muscle progenitors were present among the AFS cells, but, immediately after c-kit selection, the AFS cells' gene expression profile is not suggestive of any myogenic commitment within the transplanted population. It is noteworthy that after intravenous cell injection (and despite differences in the number of injected cells), BM- and AFS-treated animals possessed similar numbers of perinucleated fibers, highlighting the positive effect of the cell treatment. However, the functional engraftment of the two cell types in the affected muscles differs drastically and in order to explain the long-lasting effect of AFS cell transplantation, we hypothesized that the fetal cells (in contrast to BM cells) were able to migrate into the muscle stem cell niche. This behavior is a feature not only of SCs [10] but also of other stem cells of muscle origins [39] or perycites, as recently demonstrated [40]. Therefore, GFP$^+$ cells in sublaminal position warrant our theory. Despite the presence of stem cell progenitors in the BM, our selected population of fetal stem cells appears to be more efficient. In fact, 50% of the BM-treated mice and 75% of the AFS-treated mice survived for 18 months. However, only AFS-injected muscles still had a high proportion (approximately 60%) of GFP$^+$ fibers more than a year after transplantation. The high number of central nucleated fibers observed in BM-treated animals after cardiotoxin injection proved that BM cells failed to functionally integrate into the muscle stem cell niche [26, 27], whereas GFP$^+$ fibers in AFS-treated muscle resulted not only from cell fusion but also from de novo fiber generation from newly born muscle stem cells. Moreover, the higher AFS cell muscle engraftment indicated that a strong ablative preconditioning injury enhances the therapeutic effect—possibly because of the selective advantage of functionally normal cells in AFS-treated mice.

Integration of AFS cells in the stem cell niche is also confirmed by secondary transplants in *HSA-Cre, Smn*$^{F7/F7}$ of SCs isolated from BM- and AFS-treated animals. Only the latter group showed consistently the ability of giving rise to new fibers and that did not differ to the one injected with SCs derived from C57BL/6 GFP$^+$ mice. While SCs have been isolated according to a well-established protocol [10], we are limited by not using a SC lineage tracing mouse for deriving AFS cells [35].

In order to progress toward their application for therapy, it was also important to establish that AFS cell myogenic potential could be preserved or maintained after expansion, as it has been recently demonstrated for alkaline phosphatase$^+$ pericytes [32, 40]. Accordingly, expanded AFS cells intravenously injected demonstrated the maintenance of the cells' regenerative properties after culture. Twenty percent of the fibers was of donor origin, a remarkable result, given that (a) some adult stem and progenitor cells have proven difficult to expand in culture and (b) skeletal muscle SCs multiply rapidly in culture but show diminished regenerative capacity when transplanted in vivo [11]. Nevertheless, 20% was lower than the value achieved in animals having received freshly isolated cells. Further work is required to assess the relationship between myogenic potential and expansion conditions. Moreover, while it is clear that AFS cells are capable of restoring normal muscle function in *HSA-Cre, Smn*$^{F7/F7}$ mutant mice primarily by engraftment and differentiation, future

work will need to address whether paracrine function also has a role in this animal model of disease since it is possible that AFS cells could also activate resident $Pax7^+$ SCs (similarly to what has been described in BM cells) [41].

Conclusions

In conclusion, AFS cells may constitute a promising therapeutic option for muscle regeneration, since (a) systemic injection of low cell numbers clearly replenishes the muscle stem cell niche and (b) cultured AFS cells also seem to possess a high regeneration capacity. These results are relevant for the development of efficient treatment of muscle disease where an alternative to SCs is needed because of their limitation to be expanded and to migrate through the endothelial barrier. In-depth studies must be now performed with human AFS cells to verify if this new source of stem cells can open unexpected and highly required therapeutic approaches for devastating disease like those of the skeletal muscle tissue.

Acknowledgments

This work was supported by the Fondazione Città della Speranza Grants 07/02 and 10/04 and Fondazione CARIPARO Progetto di Eccellenza "Multipotentiality of fetal stem cells in a mouse model of spinal muscular atrophy." Paolo De Coppi is funded by Great Ormond Street Hospital Children's Charity. We would also like to thank Andrea Ditadi for help with establishing the isolation of amniotic fluid stem cell, Anna Cabrelle for her help with fluorescence-activated cell sorting (FACS), Mark Labrador for immunofluorescence, and Gaia Zuccolotto for in vivo imaging.

Disclosure of Potential Conflicts of Interest

The authors declare no potential conflicts of interest.

References

1 De Coppi P, Bartsch G, Jr., Siddiqui MM et al. Isolation of amniotic stem cell lines with potential for therapy. Nat Biotechnol 2007;25:100–106.
2 Grisafi D, Piccoli M, Pozzobon M et al. High transduction efficiency of human amniotic fluid stem cells mediated by adenovirus vectors. Stem Cells Dev 2008;17:953–962.
3 Ditadi A, de Coppi P, Picone O et al. Human and murine amniotic fluid c-Kit+Lin- cells display hematopoietic activity. Blood 2009;113: 3953–3960.
4 Carraro G, Perin L, Sedrakyan S et al. Human amniotic fluid stem cells can integrate and differentiate into epithelial lung lineages. Stem Cells 2008;26:2902–2911.
5 Hauser PV, De Fazio R, Bruno S et al. Stem cells derived from human amniotic fluid contribute to acute kidney injury recovery. Am J Pathol 2010;177:2011–2021.
6 Rota C, Imberti B, Pozzobon M et al. Human amniotic fluid stem cell preconditioning improves their regenerative potential. Stem Cells Dev 2011.
7 Bollini S, Pozzobon M, Nobles M et al. In vitro and in vivo cardiomyogenic differentiation of amniotic fluid stem cells. Stem Cell Rev 2011;7:364–380.
8 De Coppi P, Callegari A, Chiavegato A et al. Amniotic fluid and bone marrow derived mesenchymal stem cells can be converted to smooth muscle cells in the cryo-injured rat bladder and prevent compensatory hypertrophy of surviving smooth muscle cells. J Urol 2007;177: 369–376.
9 Gekas J, Walther G, Skuk D et al. In vitro and in vivo study of human amniotic fluid-derived stem cell differentiation into myogenic lineage. Clin Exp Med 2010;10:1–6.
10 Collins CA, Olsen I, Zammit PS et al. Stem cell function, self-renewal, and behavioral heterogeneity of cells from the adult muscle satellite cell niche. Cell 2005;122:289–301.
11 Montarras D, Morgan J, Collins C et al. Direct isolation of satellite cells for skeletal muscle regeneration. Science 2005;309:2064–2067.
12 Rossi CA, Flaibani M, Blaauw B et al. In vivo tissue engineering of functional skeletal muscle by freshly isolated satellite cells embedded in a photopolymerizable hydrogel. FASEB J 2011;25:2296–2304.
13 Galvez BG, Sampaolesi M, Brunelli S et al. Complete repair of dystrophic skeletal muscle by mesoangioblasts with enhanced migration ability. J Cell Biol 2006;174:231–243.
14 Sampaolesi M, Blot S, D'Antona G et al. Mesoangioblast stem cells ameliorate muscle function in dystrophic dogs. Nature 2006;444: 574–579.
15 Tedesco FS, Hoshiya H, D'Antona G et al. Stem cell-mediated transfer of a human artificial chromosome ameliorates muscular dystrophy. Sci Transl Med 2011;3:96ra78.
16 Dellavalle A, Sampaolesi M, Tonlorenzi R et al. Pericytes of human skeletal muscle are myogenic precursors distinct from satellite cells. Nat Cell Biol 2007;9:255–267.
17 Ghionzoli M, Cananzi M, Zani A et al. Amniotic fluid stem cell migration after intraperitoneal injection in pup rats: Implication for therapy. Pediatr Surg Int 2010;26:79–84.
18 Nicole S, Desforges B, Millet G et al. Intact satellite cells lead to remarkable protection against Smn gene defect in differentiated skeletal muscle. J Cell Biol 2003;161:571–582.
19 Sacco A, Mourkioti F, Tran R et al. Short telomeres and stem cell exhaustion model Duchenne muscular dystrophy in mdx/mTR mice. Cell 2010;143:1059–1071.
20 Salah-Mohellibi N, Millet G, Andre-Schmutz I et al. Bone marrow transplantation attenuates the myopathic phenotype of a muscular mouse model of spinal muscular atrophy. Stem Cells 2006;24:2723–2732.
21 Rossi CA, Pozzobon M, Ditadi A et al. Clonal characterization of rat muscle satellite cells: Proliferation, metabolism and differentiation define an intrinsic heterogeneity. PLoS One 2010;5:e8523.
22 Blaauw B, Mammucari C, Toniolo L et al. Akt activation prevents the force drop induced by eccentric contractions in dystrophin-deficient skeletal muscle. Hum Mol Genet 2008;17:3686–3696.
23 Silletti A, Cenedese A, Abate A. The emergent structure of the drosophila wing—A dynamic model generator: Proceedings of the 4th International Conference on Computer Vision Theory and Applications (Visapp), 2009;1:406–410.
24 Ferrari G, Cusella-De Angelis G, Coletta M et al. Muscle regeneration by bone marrow-derived myogenic progenitors. Science 1998;279:1528–1530.
25 Gussoni E, Soneoka Y, Strickland CD et al. Dystrophin expression in the mdx mouse restored by stem cell transplantation. Nature 1999; 401:390–394.
26 Xynos A, Corbella P, Belmonte N et al. Bone marrow-derived hematopoietic cells undergo myogenic differentiation following a Pax-7 independent pathway. Stem Cells 2010;28:965–973.
27 Sherwood RI, Christensen JL, Conboy IM et al. Isolation of adult mouse myogenic progenitors: Functional heterogeneity of cells within and engrafting skeletal muscle. Cell 2004;119:543–554.
28 Choi J, Costa ML, Mermelstein CS et al. MyoD converts primary dermal fibroblasts, chondroblasts, smooth muscle, and retinal pigmented epithelial cells into striated mononucleated myoblasts and multinucleated myotubes. Proc Natl Acad Sci USA 1990;87:7988–7992.
29 De Bari C, Dell'Accio F, Vandenabeele F et al. Skeletal muscle repair by adult human mesenchymal stem cells from synovial membrane. J Cell Biol 2003;160:909–918.
30 Goudenege S, Pisani DF, Wdziekonski B et al. Enhancement of myogenic and muscle repair capacities of human adipose-derived stem cells with forced expression of MyoD. Mol Ther 2009;17:1064–1072.
31 Parker MH, Kuhr C, Tapscott SJ et al. Hematopoietic cell transplantation provides an immune-tolerant platform for myoblast transplantation in dystrophic dogs. Mol Ther 2008;16:1340–1346.
32 Sampaolesi M, Torrente Y, Innocenzi A et al. Cell therapy of alpha-sarcoglycan null dystrophic mice through intra-arterial delivery of mesoangioblasts. Science 2003;301:487–492.
33 Diaz-Manera J, Touvier T, Dellavalle A et al. Partial dysferlin reconstitution by adult murine mesoangioblasts is sufficient for full functional recovery in a murine model of dysferlinopathy. Cell Death Dis 2010;1:e61.
34 Sakurai H, Okawa Y, Inami Y et al. Paraxial mesodermal progenitors derived from mouse embryonic stem cells contribute to muscle regeneration via differentiation into muscle satellite cells. Stem Cells 2008;26:1865–1873.
35 Darabi R, Gehlbach K, Bachoo RM et al. Functional skeletal muscle regeneration from differentiating embryonic stem cells. Nat Med 2008;14:134–143.

36 Takahashi K, Tanabe K, Ohnuki M et al. Induction of pluripotent stem cells from adult human fibroblasts by defined factors. Cell 2007; 131:861–872.

37 Darabi R, Pan W, Bosnakovski D et al. Functional myogenic engraftment from mouse iPS cells. Stem Cell Rev 2011;7:948–957.

38 Mizuno Y, Chang H, Umeda K et al. Generation of skeletal muscle stem/progenitor cells from murine induced pluripotent stem cells. FASEB J 2010;24:2245–2253.

39 Cerletti M, Jurga S, Witczak CA et al. Highly efficient, functional engraftment of skeletal muscle stem cells in dystrophic muscles. Cell 2008;134:37–47.

40 Dellavalle A, Maroli G, Covarello D et al. Pericytes resident in postnatal skeletal muscle differentiate into muscle fibres and generate satellite cells. Nat Commun 2011;2:499.

41 Yoon BS, Moon JH, Jun EK et al. Secretory profiles and wound healing effects of human amniotic fluid-derived mesenchymal stem cells. Stem Cells Dev 2010;19:887–902.

See www.StemCells.com for supporting information available online.